

Determination of reactivity ratios for the copolymerization of poly(acrylic acid-co-itaconic acid)

Shidan Cummings,¹ Yujie Zhang,¹ Niousha Kazemi,² Alexander Penlidis,² Marc A. Dubé¹

¹Department of Chemical & Biological Engineering, University of Ottawa, Ottawa, ON K1N 6N5, Canada

²Department of Chemical Engineering, University of Waterloo, Waterloo, ON N2L 3G1, Canada

Correspondence to: M. A. Dubé (E-mail: marc.dube@uottawa.ca)

ABSTRACT: Monomer reactivity ratios are important parameters used in copolymerization kinetics to predict the rate of polymerization, copolymer composition and monomer sequence length, and by extension, molecular weight and distribution of the final product. Batch aqueous solution copolymerizations of acrylic acid (AA) and itaconic acid (IA) are performed at various feed compositions. Polymerizations are categorized into low (<11 wt %) conversion and higher (<30 wt %) conversion data sets for analysis. Due to the limited solubility of IA in the reaction mixture, the feed composition of IA in all polymerizations is constrained to lower than 25 mol %. Conversion is determined by gravimetric methods, and copolymer composition via ¹H-NMR spectroscopy. All data are analyzed using the error-in-variables model (EVM) method. Two analyses are used, one with the EVM approach and another with a novel Direct Numerical Integration (DNI) coupled with the EVM method. The DNI/EVM approach yields values of $r_{AA} = 0.36$ and $r_{IA} = 1.62$ for the reactivity ratios. © 2016 Wiley Periodicals, Inc. *J. Appl. Polym. Sci.* **2016**, *133*, 44014.

KEYWORDS: biomaterials; copolymers; kinetics; radical polymerization

Received 7 November 2015; accepted 2 June 2016

DOI: 10.1002/app.44014

INTRODUCTION

Bioadhesives are polymers that adhere to a biological substrate, typically a tissue or membrane, for the purposes of bonding two materials together, often to promote the healing of a damaged tissue. The bioadhesive must be able to wet the surface to be effective; this is followed by permeation of the polymer matrix into the substrate and the eventual formation of an adhesive bond. Anionic polymers are good candidates to be used as bioadhesives because they often exhibit electrostatic attraction as well as hydrogen bonding, which improve wetting and adhesion to mucus membranes.

Poly(acrylic acid) (PAA) is an anionic polymer, currently a popular bioadhesive for the delivery of various medicinal ingredients including peptides, hydrophilic drugs, and calcium ions.^{1–4} While only oligomers of PAA are biodegradable, acrylic acid (AA)-based hydrogels have extremely good adhesive and drug delivery properties because of their hydrophilic nature and abundance of carboxyl groups, and are often used as a backbone in copolymers with biodegradable components.^{5–7} One potential comonomer that is biodegradable is itaconic acid (IA). The structure of IA includes two carboxyl groups that readily oxidize and act as attack sites for enzymatic degradation. Therefore, IA is a viable candidate for copolymerization with AA to increase the degradation rate of the bioadhesive.⁸ IA is a naturally occur-

ring, non-toxic, and readily biodegradable white crystalline powder. Interest in IA was rekindled when it was found that it could be produced in substantial quantities by means of a fermentation process; it is currently produced by the fermentation of carbohydrates such as glucose.⁹ The most common application of IA-based polymers is in the form of glass-ionomer dental restoratives,¹⁰ in hydrogel grafts for oral drug delivery,¹¹ and in the paint, textile, adhesive, plastic molding, and paper coating industries.¹² Notably, IA has limited solubility in water at 0.2467 g mL⁻¹ at 97 °C.¹⁰ Figure 1 shows the typical structure of poly(AA-co-IA), where the introduction of carboxyl groups on both sides of the polymer chain by incorporation of IA can be seen.

In this article, we wish to synthesize a polymeric bioadhesive with the ability to have its degradation rate modified. This adhesive will be used on various human tissues. Depending on the physical properties of the particular tissue, the degradation rate will need to be adjusted so that the polymer degrades safely and at an appropriate rate for drug/active ingredient delivery for a broad range of applications.¹³ In order for the polymer chain to have the desired composition, and thus a tunable degradation rate based on what monomer units have been incorporated in the copolymer chains, the monomer reactivity ratios need to be determined as a first step. Monomer reactivity ratios

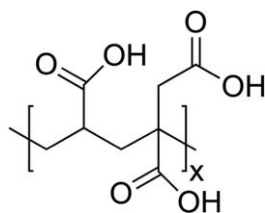


Figure 1. Poly(AA-co-IA) molecule.

are important parameters used in copolymerization kinetics to predict the rate of polymerization, copolymer composition and monomer sequence length, and by extension, molecular weight and distribution of the final product.^{14,15}

Reactivity Ratios

The composition of polymer chains in a free radical copolymerization, unlike those in step growth polymerization, is not necessarily the same as the composition of the comonomer feed. In chain growth copolymerization, the two monomers enter the polymer chain in amounts determined by their relative reactivities (and, of course, available concentrations). The reactivity ratios are parameters in a copolymer composition model that represent the relative reactivities of the two monomers and their radical counterparts.

The terminal model for copolymerization makes the assumption that the chemical reactivity of the propagating chain in a copolymerization is dependent solely on the identity of the monomer unit at the propagating end of the chain, and not on any of the preceding monomer units. For a copolymerization with two monomers, M_1 and M_2 , where the propagating radical unit is M_1^* and M_2^* , there are four possible propagation reactions. The reactivity ratios can be expressed in terms of the reaction rate constants of these four reactions:

$$r_1 = \frac{k_{11}}{k_{12}} \quad (1)$$

$$r_2 = \frac{k_{22}}{k_{21}} \quad (2)$$

The rates of entry of the monomers into the copolymer, synonymous with their removal from the monomer mixture, are:

$$-\frac{d[M_1]}{dt} = k_{11}[M_1^*][M_1] + k_{21}[M_2^*][M_1] \quad (3)$$

$$-\frac{d[M_2]}{dt} = k_{12}[M_1^*][M_2] + k_{22}[M_2^*][M_2] \quad (4)$$

Using eqs. (3) and (4), the Mayo–Lewis equation, known also as the instantaneous copolymer composition model, can be derived as:

$$\frac{F_1}{F_2} = \frac{(r_1 f_1 + f_2) f_1}{(f_1 + r_2 f_2) f_2} \quad (5)$$

An alternative, and probably more useful form of eq. (5), is expressed as:

$$F_1 = \frac{r_1 f_1^2 + f_1 f_2}{f_1 f_1^2 + 2f_1 f_2 + r_2 f_2^2} \quad (6)$$

where F_1 and F_2 are the instantaneous mole fractions of monomers 1 and 2 (incorporated, bound) in the copolymer, respec-

tively; f_1 and f_2 are the mole fractions of monomers 1 and 2 in the reaction mixture, respectively; and r_1 and r_2 are the monomer reactivity ratios. F and f change, in general, with polymerization time/conversion.

The monomer feed and copolymer composition must be known for the estimation of the reactivity ratios. Because of the tendency of copolymer composition to drift (and often significantly, due to differing monomer reactivities), one must record the overall monomer conversion. Traditionally, to avoid bias due to composition drift, reactions are run to low conversions (typically, <5–10 wt %) for reactivity ratio determination. Copolymer composition can be determined using various techniques but the most common and also for the purposes of this article, proton nuclear magnetic resonance (¹H-NMR) spectroscopy was used.

pH Dependence

Gao *et al.* and Riahinezhad *et al.* presented a thorough examination of the strong pH-dependent characteristics in polymerizations involving AA showing a trend of decreasing polymerization rate with increasing pH above a value of 1, where the rate is at a maximum (in the range of $0 < \text{pH} < 7$).^{16,17} IA shows similar pH/ionization dependence, as the rate of homopolymerization is reported to be constant at $\text{pH} < 3.8$ and virtually zero at $\text{pH} > 4.4$. It would follow that the reactivity ratios for the AA/IA copolymerization are also a function of pH. As pH increases, the reactivity ratio, r_{1A} , should decrease due to the increasing difficulty for the di-anion of IA to propagate.¹¹ It may be noted that at neutral pH, PAA and PIA become deprotonated and can absorb a large amount of water, swelling to many times their original size.

Since the pH dependence of AA is as a result of its carboxyl groups, it would follow that a system comprising AA and IA monomers would be very susceptible to such a dependency.^{11,16,17} IA has two carboxyl groups, and with pK values of 3.85 and 5.45 (lower than the carboxyl group of AA), the pH of the reaction mixture would need to be lower to maintain a high polymerization rate.

EXPERIMENTAL

Materials

AA in liquid form (99%; Sigma-Aldrich) and IA as a solid powder (99+% ; Sigma-Aldrich) were used with no further purification. Azobisisobutyronitrile (AIBN) was used as initiator and was recrystallized three times in methanol (Sigma-Aldrich). Distilled, de-ionized (DDI) water was used throughout the experiment as solvent. “Baker” grade hydroquinone solution (JT Baker) and technical grade methyl ethyl ketone (MEK) (Fisher Scientific) were used as received.

Procedure

The polymerizations were performed in a 500 mL glass RC1e reactor (Mettler–Toledo). The appropriate amount of DDI water, IA, and AA was charged to the reactor under nitrogen sparging. The total mass of reactants in every polymerization was maintained at 300 g to ensure similar mixing conditions. After the IA was dissolved, the reaction mixture was heated to

50°C. The initiator (0.0003 g/g monomer) was then charged to start the polymerization.

A septum was used to sample the reaction mixture during polymerization for the measurement of monomer conversion and copolymer composition. A total of 10 mL samples were drawn, weighed, and immediately placed in pre-weighed centrifuge tubes. The reaction was terminated by adding <1 mL of hydroquinone solution to the tube.

MEK was added to each sample at a 2:1 (vol/vol) ratio to precipitate the polymer and remove the unreacted solid IA and liquid AA. Samples were then centrifuged at 6000 rpm for 20 min, at which point the IA-rich MEK solution was decanted. Samples were first dried at room temperature, then vacuum-dried until a constant sample weight was achieved.

¹H-NMR spectroscopic analysis, using a Bruker AVANCE II 400 spectrometer with sample charger (400 MHz), was conducted on each sample to measure the copolymer composition. The sample solutions were prepared by mixing a small amount of dry polymer with D₂O in a glass vial at a concentration of ~0.02 g sample/1.5 g D₂O. The polymer was allowed to dissolve for 24 h to ensure its sufficient dissolution. Pure samples of AA, IA, and PAA were also analyzed in order to assist with peak identification in the copolymer spectra. Sample conversion was determined by gravimetry based on the amount of dried polymer recovered and corrected for residual IA, AA, and MEK in the polymer determined by ¹H-NMR spectroscopy.

Estimation and Experimental Design

The Mayo–Lewis equation [eqs. (5) and (6)] is a highly nonlinear equation. Despite this, several inaccurate linearization methods for reactivity ratio determination persist in the scientific literature, for example, Fineman–Ross (see the discussion in references^{18–20} for more details). The most statistically sound methods for reactivity ratio determination, however, are nonlinear. The nonlinear least squares (NLLS) method and the more advanced error-in-variables-model (EVM) method have been available for decades and have repeatedly been shown to be more appropriate for use with the nonlinear Mayo–Lewis model. The EVM method was used for the purposes of this study.^{20–22}

The typical approach to using the EVM method for reactivity ratio determination consists of (1) maintaining low conversion (typically, <10 wt %) to avoid composition drift, (2) conducting a set of runs at equidistant feed compositions to calculate initial reactivity ratio estimates, and (3) using the Tidwell–Mortimer criterion to design an additional set of replicated experiments at two new compositions.

A novel approach developed by Kazemi *et al.*^{20–22} was implemented herein and consists of an extension of the typical EVM method to allow for the use of moderate or high conversion data in the reactivity ratio estimation. The approach, termed Direct Numerical Integration (DNI), uses the integrated form of the Mayo–Lewis equation. Thus, experiments to higher conversions are performed and the entire data set (i.e., not only information from low conversion levels) is used. Furthermore, the approach employed by Kazemi *et al.*^{20–22} enables one to design

the next best set of experiments to achieve accurate reactivity ratios. The approach, termed EVM-based design criterion (an extension of the well-known D-optimality criterion), also allows for the use of a constrained design space. This method was particularly appropriate for the current case given the solubility limit of IA.

Because the reactivity ratios of this system are expected to be pH dependent, the set of experiments were run at 75, 83, and 90 mol % AA at 39 wt % monomer concentration and relatively constant pH of 1.65. Multiple polymerizations at various compositions are required to generate accurate estimates of the reactivity ratios. It should be noted that by varying the AA concentration relative to IA, the pH of the reaction mixture will change across the entire set of experimental runs. This difference in pH was unavoidable as no buffer was used to avoid possible kinetic effects. Nonetheless, the pH was kept within the relatively narrow range of ±0.5.

RESULTS AND DISCUSSION

Experimental Challenges

The homo- and copolymerization of any system containing AA and IA will be pH dependent. The reactivity ratios, then, should be taken to be dependent on the initial pH of the reaction mixture and the reaction rate. The polymerization of IA is hindered by the presence of allylic hydrogens, which will increase the risk of degradative chain transfer. Maintaining the pH as close to 1 as possible mitigates this chain transfer.^{11,23} The solubility of IA in water limits our ability to carry out polymerizations at high IA incorporation, which limits our feed composition design. The separation of unreacted IA was difficult because it is a solid at room temperature and although MEK was used to separate the dried monomer, ¹H-NMR analysis revealed that some traces of IA remained in the polymer samples after this process. ¹H-NMR peaks of the pure AA monomer and final copolymer also revealed the presence of di-acrylic acid (DAA) and poly(di-acrylic acid) (PDAA). The presence of IA, DAA, and PDAA further complicated the determination of conversion and composition data.

Conversion

Conversion vs. time data for each of the three runs are shown in Figure 2. The symbol *f* in Figure 2 (and elsewhere in the paper) denotes initial mole fraction of AA in the feed. Residual monomer (i.e., IA and AA) and solvent (i.e., MEK) were identified in most samples via ¹H-NMR analysis and were used to correct the sample conversion data.

¹H-NMR Peak Analysis

The analysis of ¹H-NMR peaks was challenging due to the high degree of overlap of polymer peaks as well as the peaks from residual IA, AA, DAA, and MEK. Figure 3(a) and Table I show the peak assignments,^{9,24–26} while Figure 3(b) shows the protons used to calculate the copolymer composition. Peaks A–D, F, H, I, and K in Table I are shown for completeness but were not necessary for copolymer composition calculation. The area under peak J represents two PAA protons (because the PDAA and PAA overlapped in peak J, both sets of protons were considered as PAA for conversion and composition calculations).

The area under peak G represents two PIA protons along with two DAA and two PDAA protons. Subtracting the area under peak E (two DAA and two PDAA protons) from peak G gives

$$\text{mol\% PAA} = \left(\frac{\text{Area under peak J}}{2 \text{ protons}} / \frac{\text{Area under peak G} - \text{Area under peak E} + \text{Area under peak J}}{4 \text{ protons}} \right) \times 100 \quad (7)$$

Reactivity Ratio Determination

An EVM reactivity ratio estimator originally developed by Dubé *et al.*¹⁴ and later enhanced by Polic *et al.*¹⁸ was initially used to calculate the reactivity ratios. This program uses the initial feed composition and the final copolymer composition of one of the monomers (in our case, AA) to estimate the reactivity ratios. Data points from conversions above 10 wt % were not included in the analyses and thus, a total of 21 data points were used (see Table II). The symbol F in Table II represents cumulative copolymer composition (mole fraction of monomer units bound in the copolymer). In the second estimation stage, all 26 data points through all conversions were used for analysis using the modified EVM method of Kazemi *et al.*^{20–22} The results for the low conversion analysis by EVM and the full conversion analysis by DNI/EVM approach were ($r_1 = 0.41$, $r_2 = 1.84$) and ($r_1 = 0.36$, $r_2 = 1.62$), respectively, where monomer 1 is AA and monomer 2 is IA. The 95% joint confidence region (JCR) is shown in Figure 4. The JCR is a very useful measure of the uncertainty (variability, variance) of the point estimates of the parameters in question; the larger the area of the JCR, the larger the variability (uncertainty).

The data analyzed by the DNI/EVM method should theoretically produce a smaller JCR for the reactivity ratio estimates. Because of the error associated with the calculation of conversion values for systems containing IA, implementation of the DNI method (i.e., expansion into higher conversion levels which contained more error) had a negative effect on the accuracy of the estimates. Despite this negative effect on the overall

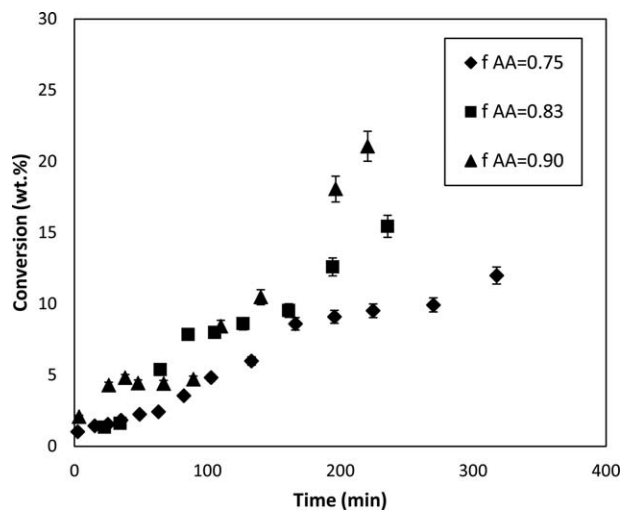


Figure 2. Conversion vs. time data.

the area equivalent to two PIA protons. Finally, the mole percent of PAA bound in the copolymer is calculated using

measure of certainty (of the JCRs), the point estimates were still very similar.

The cumulative AA copolymer composition (F_1 or F_{AA}) was plotted against conversion as shown in Figures 5 and 6. The reactivity ratios from the DNI/EVM method ($r_{AA} = 0.36$ and $r_{IA} = 1.62$) were used because predictions from both sets of point estimates yielded statistically identical results. In any case, as shown in Figure 4, the point estimates are not statistically different. Thus, the reactivity ratio point estimates yielded composition vs. conversion curves that fit the set of data extremely well, as seen in Figure 6, for the three monomer feed compositions studied. The cumulative copolymer composition is related to the incorporated monomer units in the copolymer chains from the start of the polymerization to the measured time (as opposed to the instantaneous copolymer composition, which is related to the monomer units incorporated in the copolymer chains over an infinitesimal time period). Given the low conversion values of all data points, only a small degree of composition drift was observed, as expected, in both the cumulative and instantaneous copolymer composition curves. It is not surprising then, that both methods for determining the reactivity ratios produced statistically similar point estimates, regardless of the error associated with the higher conversion data points included in the DNI/EVM method.

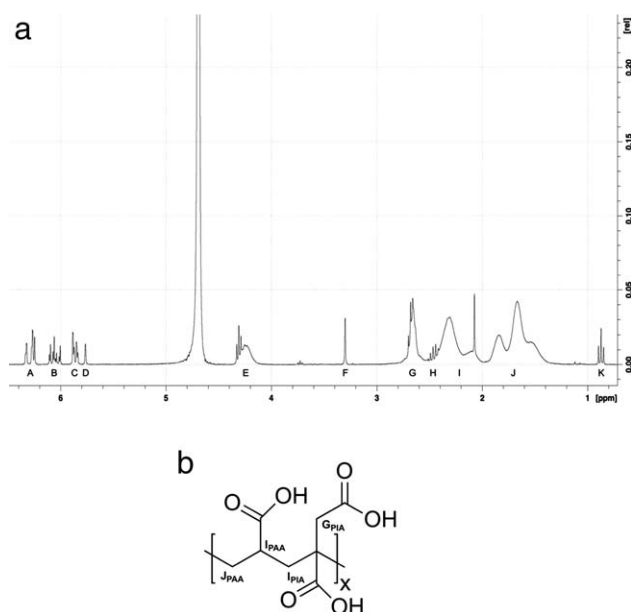


Figure 3. (a) AA/IA copolymer ¹H-NMR peak identification. Sample composition: 83 mol % AA. (b) Proton identification of AA/IA copolymer.

Table I. NMR Peak Assignments

Peak label	Region	Species	Protons	Peak area ^a
A	6.2–6.4	AA/DAA IA	1 1	1.00
B	6.0–6.2	AA/DAA	1	0.72
C	5.8–6.0	AA/DAA	1	0.81
D	5.7–5.8	IA	1	0.23
E	4.0–4.4	DAA/PDAA	2	2.46
F	3.3–3.5	IA	2	0.46
G	2.6–2.8	DAA/PDAA PIA	2 2	3.96
H	2.4–2.5	MEK	2	1.01
I	2.0–2.4	PIA PAA/PDAA MEK	2 1 3	8.09
J	1.4–2.0	PAA/PDAA	2	12.33
K	0.8–1.0	MEK	3	0.47

^aPeak areas correspond to Figure 3(a).

Table II. Conversion Data

Initial composition	Conversion (wt %)	F_{AA} (mole fraction)	F_{IA} (mole fraction)
$f_{AA} = 0.7505$	2.25	0.6006	0.3604
	2.42	0.6061	0.3939
	3.56	0.5750	0.4250
	4.82	0.5756	0.4244
	5.99	0.5662	0.4338
	8.60	0.5683	0.4317
	9.10	0.5734	0.4266
	9.52	0.5820	0.4180
	9.93	0.5755	0.4245
$f_{AA} = 0.83$	1.34	0.7174	0.2826
	1.61	0.6777	0.3223
	5.38	0.6801	0.3199
	7.85	0.6913	0.3087
	7.99	0.6851	0.3149
	8.61	0.7004	0.2996
	9.53	0.6951	0.3049
	12.59	0.6831	0.3169
	15.44	0.6786	0.3214
	$f_{AA} = 0.90$	4.81	0.7795
4.43		0.8140	0.1860
4.40		0.7910	0.2090
4.69		0.7846	0.2154
8.43		0.7874	0.2126
10.47		0.7816	0.2184
18.06		0.7852	0.2148
21.07	0.7772	0.2228	

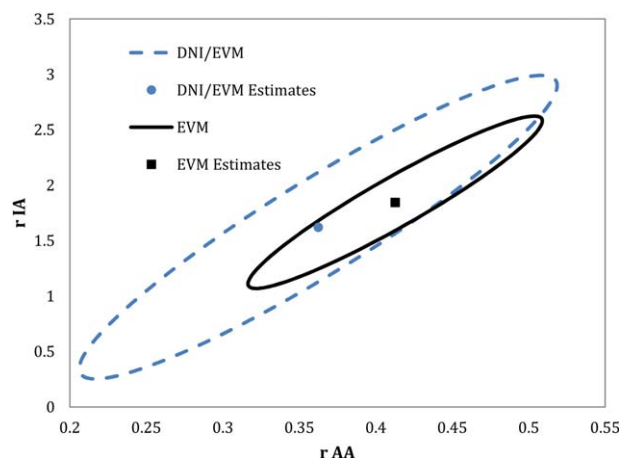


Figure 4. 95% Joint confidence regions (data of Table II). [Color figure can be viewed in the online issue, which is available at wileyonlinelibrary.com.]

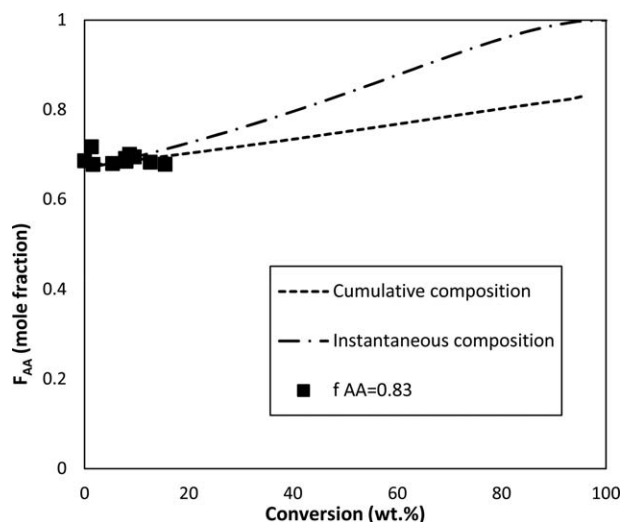


Figure 5. Cumulative and instantaneous copolymer composition for AA feed composition of 0.83 mole fraction.

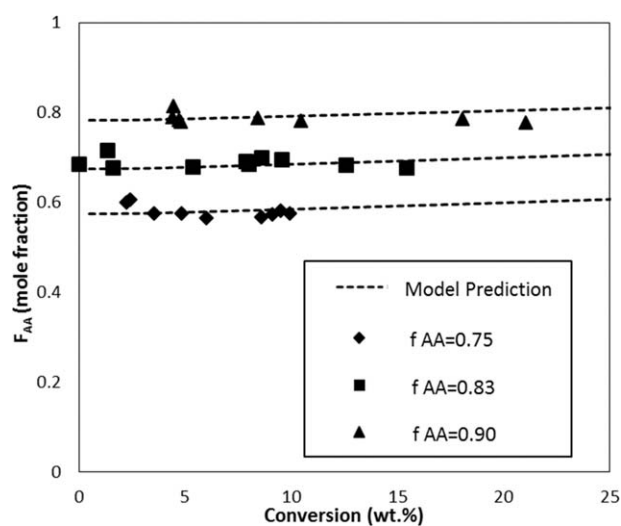


Figure 6. Cumulative copolymer composition vs. conversion.

CONCLUSIONS

The EVM approach for reactivity ratio estimation was successfully applied to the copolymerization of AA and IA in aqueous solution (a rather noisy copolymerization due to the nature of the system). Challenges with conversion and composition determination due to $^1\text{H-NMR}$ peak overlap and poor separation of residual itaconic acid were discussed. Despite these experimental issues, both the EVM and DNI/EVM approaches, being able to take properly into account the error in all variables involved, were able to generate point estimates of the reactivity ratios as $r_{AA} = 0.41$ and $r_{IA} = 1.84$ and $r_{AA} = 0.36$, $r_{IA} = 1.62$, respectively. It was expected that the DNI/EVM method, taking into account higher conversion data, would provide more precise and more accurate point estimates for the reactivity ratios, however this was not possible given the difficulties in determining accurate conversion values for the system. Given that the limitations of the system did not allow for conversions above 21 wt % nor feed compositions below $f_{AA} = 0.75$ mole fraction (for the water concentration studied), the additional error associated with the conversion and composition calculations did not impact the accuracy of the DNI/EVM point estimate, but the precision was affected. Regardless, both sets of reactivity ratios yielded statistically identical cumulative and instantaneous copolymer composition predictions.

ACKNOWLEDGMENTS

The authors gratefully acknowledge the financial support of the Natural Sciences and Engineering Research Council (NSERC) of Canada.

REFERENCES

1. Kriwet, B.; Walter, E.; Kissel, T. *J. Control. Rel.* **1998**, *56*, 149.
2. Kriwet, B.; Kissel, T. *J. Pharm.* **1996**, *127*, 135.
3. Anlar, S.; Capan, Y.; Hincal, A. *Pharmazie* **1993**, *48*, 285.
4. Laulicht, B.; Mancini, A.; Geman, N.; Cho, D.; Estrellas, K.; Furtado, S.; Hopson, R.; Tripathi, A.; Mathiowitz, E. *Macromol. Biosci.* **2012**, *12*, 1555.
5. Hu, Y.; Jiang, X.; Ding, Y.; Ge, H.; Yuan, Y.; Yang, C. *Biomaterials* **2002**, *23*, 3193.
6. Pourjavadi, A.; Barzegar, S.; Zeidabadi, F. *React. Funct. Polym.* **2007**, *67*, 644.
7. Gao, X.; He, C.; Xiao, C.; Zhuang, X.; Chen, X. *Mater. Lett.* **2012**, *77*, 74.
8. Chandra, R.; Rustgi, R. *Prog. Polym. Sci.* **1998**, *23*, 1273.
9. Cowie, J. *Pure Appl. Chem.* **1979**, *51*, 2331.
10. Culbertson, B.; Dotrong, M. *J. Macromol. Sci., Part A: Pure Appl. Chem.* **2007**, *37*, 2000.
11. Betancourt, T.; Pardo, J.; Soo, K.; Peppas, N. *J. Biomed. Mater. Res. A* **2011**, *93*, 175.
12. El-Imam, A.; Du, C. *J. Biodivers. Biopros. Dev.* **2014**, *1*, 119.
13. Liechty, W.; Kryscio, D.; Slaughter, B.; Peppas, N. *Ann. Rev. Chem. Biomol. Eng.* **2010**, *1*, 149.
14. Dubé, M.; Sanayei, R.; Penlidis, A.; O'Driscoll, K.; Reilly, P. *A. J. Polym. Sci., Part A: Polym. Chem.* **1991**, *29*, 703.
15. Gao, J.; Penlidis, A. *J. Macromol. Sci.-Revs. Macromol. Chem. Phys.* **1998**, *38*, 651.
16. Gao, J.; Penlidis, A. *J. Macromol. Sci.-Revs. Macromol. Chem. Phys.* **1996**, *36*, 199.
17. Riahinezhad, M.; McManus, N.; Penlidis, A. *Macromol. React. Eng.* **2014**, DOI: 10.1002/mren.201400053.
18. Polic, A.; Duever, T.; Penlidis, A. *J. Polym. Sci., Part A: Polym. Chem.* **1998**, *36*, 813.
19. Hauch, E.; Zhou, X.; Duever, T.; Penlidis, A. *Macromol. Symp.* **2008**, *1*, 48.
20. Kazemi, N.; Duever, T.; Penlidis, A. *Macromol. Theory Simul.* **2013**, *22*, 261.
21. Kazemi, N.; Duever, T.; Penlidis, A. *Macromol. React. Eng.* **2011**, *5*, 385.
22. Kazemi, N.; Duever, T.; Penlidis, A. *Comp. Chem. Eng.* **2013**, *48*, 200.
23. Stawski, D.; Polowinski, S. *Polimery* **2005**, *50*, 118.
24. Gottlieb, H.; Kotlyar, V.; Nudelman, A. *J. Org. Chem.* **1997**, *62*, 7512.
25. Rosendo, A.; Flores, M.; Cordoba, G.; Rodriguez, R.; Arroyo, R. *Mater. Lett.* **2003**, *57*, 2885.
26. Wishart, D. S.; Knox, C.; Guo, A. C.; Eisner, R.; Young, N.; Gautam, B.; Hau, D. D.; Psychogios, N.; Dong, E.; Bouatra, S.; Mandal, R.; Sinelnikov, I.; Xia, J.; Jia, L.; Cruz, J. A.; Lim, E.; Sobsey, C. A.; Shrivastava, S.; Huang, P.; Liu, P.; Fang, L.; Peng, J.; Fradette, R.; Cheng, D.; Tzur, D.; Clements, M.; Lewis, A. D.; Souza, A.; Zuniga, A.; Dawe, M.; Xiong, Y.; Clive, D.; Greiner, R.; Nazyrova, A.; Shaykhtudinov, R.; Li, L.; Vogel, H. J.; Forsythe, I. *Nucleic Acids Res.* **2009**, *37*, D603.